Effects of Rate Adaptation on the Throughput of Random Ad Hoc Networks

Xiang Liu and Lajos Hanzo

School of ECS, University of Southampton, SO17 1BJ, UK.
Tel: +44-23-8059-3125, Fax: +44-23-8059-4508
Email:lh@ecs.soton.ac.uk, http://www-mobile.ecs.soton.ac.uk

Abstract

The capacity of wireless *ad hoc* networks has been studied in an excellent treatise by Gupta and Kumar [1], assuming a *fixed transmission rate*. By contrast, in this treatise we investigate the achievable throughput improvement of *rate adaptation* in the context of random *ad hoc* networks, which have been studied in conjunction with a *fixed transmission rate* in [1]. Our analysis shows that *rate adaptation* has the potential of improving the achievable throughput compared to *fixed rate transmission*, since *rate adaptation* mitigates the effects of link quality fluctuations. However, even perfect rate control fails to change the scaling law of the per-node throughput result given in [1], regardless of the absence or presence of shadow fading. This result is confirmed in the context of specific adaptive modulation aided design examples.

1. INTRODUCTION

An *ad hoc* network consists of a number of mobile nodes, which may communicate directly with each other over wireless links, but an *ad hoc* network has no base station infrastructure. One of the most important characteristics of *ad hoc* networks is their *achievable capacity* [1]. More specifically, in their landmark paper [1] Gupta and Kumar studied the achievable capacity of *ad hoc* networks having n nodes, each capable of transmitting at W bits per second. Two types of network models were considered in their work, *arbitrary networks*, which consist of arbitrarily located nodes generating an arbitrary traffic pattern, and *random networks*, which consist of randomly located nodes generating a random traffic pattern. The results of [1] showed that the throughput achievable by each node was $\Theta(W/\sqrt{n})$[1] for *arbitrary networks* and $\Theta(W/\sqrt{n\log n})$ for *random networks*. Both of these formulae implied that the per-node throughput tended to zero, as the number of nodes tended to infinity.

Directional and other types of smart antennas have also been used for increasing the achievable capacity of wireless *ad hoc* networks [2,3]. It was shown [2,3] that the *scalability* problem[2] might be mitigated by increasing the number of antenna elements and the resultant antenna gain, which is a benefit of having a narrower beam-width. However, despite its considerable complexity, beamforming does not dramatically change the scaling law[3] due to the limitations of realistic systems [3].

It was also shown [5] that terminal mobility was capable of increasing the per-node throughput to $\Theta(1)$ with the aid of a two-hop strategy, even when the number of communicating nodes n was high, provided that the transmission delay was not taken into account, which is a somewhat irrealistic assumption. However, the expected delay per packet imposed by the above strategy might be $\Theta(\log n)$ [6], which suggests that mobile *ad hoc* networks constituted by many nodes may not be scalable in real-time applications.

The capacity of hybrid wireless networks, which consist of *ad hoc* nodes benefitting from infrastructure support, was studied in [7,8]. The results showed that the per-node throughput of *ad hoc* networks was improved by the infrastructure support provided by both regular base stations [7] and random distributed access points [8].

A mathematical framework was defined for studying the capacity of wireless *ad hoc* networks in [9]. The results showed that multihop routing, spatial reuse[4], successive interference cancellation (SIC) and variable-rate transmissions hold the promise of significantly improving the achievable capacity. Both terminal mobility and fading were also found to increase the achievable network capacity, provided that nodes were capable of tolerating large delays, since the network was allowed to schedule its transmissions during favourable fading or mobility conditions.

In most of the above mentioned literature, a *fixed transmission rate* associated with a time-invariant modulation scheme was assumed [1–3,5,7,8]. Toumpis and Goldsmith numerically characterized the effects of *rate adaptation* with the aid of a rigorous mathematical framework [9], stating that the associated computational complexity of scheduling would increase exponentially, as the number of nodes increased.

In this paper, the effect of *rate adaptation* on the achievable per-node throughput of *ad hoc* networks will be estimated. In Section 2, the system model of wireless *ad hoc* networks is introduced. In Section 3, the achievable throughput improvements of perfect *rate adaptation* are estimated without taking into account the effects of fading. To expound further, in Section 4 the effect of perfect *rate adaptation* under shadowing is analyzed. Examples of Adaptive Quadrature Amplitude Modulation (AQAM) simulations are provided in Section 5. Finally, Section 6 provides our conclusions.

The financial support of the European Union under the auspices of the Phoenix and Newcom projects as well as of the EPSRC, UK is gratefully acknowledged.

[1]The function $\Theta(W/\sqrt{n})$ returns a value, which is not much worse, but also not much better than $W/\sqrt{n}$.

[2]Scalability in *ad hoc* networks implies that whether the network is capable of providing an acceptable level of service, when the number of nodes in the network tends to infinity [4].

[3]The scaling law in *ad hoc* networks characterizes how the network performance varies, as the number of nodes in the network tends to infinity. In this treatise the network performance is measured by the achievable per-node throughput.

[4]Spatial reuse implies that more than one nodes are allowed to attempt the simultaneous transmission of a given packet towards its destination.

2. SYSTEM MODEL

Our model of the *ad hoc* network considered is similar to that used in [1], apart from a few modifications, which include the employment of perfect *rate adaptation* and the effects of a fading channel.

Let us consider a random *ad hoc* network supporting n nodes uniformly and independently distributed in a unit area $\mathcal{S}$, which is a planar disk as in [1]. All nodes share the same bandwidth, which is given by W Hz. All packet-transmissions are slotted into perfectly synchronized time slots. No node is capable of simultaneously transmitting and receiving signals, or simultaneously transmitting/receiving signals to/from more than one node. The power of each transmitting node is fixed to P_t Watts, i.e. no power control is used, which is typical in cost-efficient *ad hoc* networks.

Let $\mathcal{N}_t$ be the subset of nodes simultaneously transmitting at some time instant. If node i, $i \notin \mathcal{N}_t$ is receiving signals from node j, $j \in \mathcal{N}_t$, then the Signal-to-Interference-plus-Noise Ratio (SINR) experienced at node i becomes:

$$\gamma_{ji} = \frac{P_t G_{ji}}{\sum_{k\in\mathcal{N}_t, k\neq j} P_t G_{ki} + \eta_i}, \quad (1)$$

where γ_{ji} is the SINR at node i experienced by the signal arriving from node j, while G_{ki} is the power gain between nodes k and i, while η_i is the background noise encountered at node i. The value of the power gain G_{ji} depends on the propagation model, which will be discussed in Sections 3 and 4, taking into account the absence of fading or the presence of log-normal shadow fading, respectively. The minimum SINR required for successful reception is β, as defined in [1].

Every transmitting node assumes perfect knowledge of its link quality and hence we are estimating the achievable throughput upper bound with the advent of perfect adaptive rate transmission, which is a prerequisite for approaching the Shannon limit [10].

The common reliable transmission range $r(n)$ of all nodes is chosen to guarantee the asymptotic connectivity of random networks as in [1]. The shorthand of r_n will be used for $r(n)$ in the sequel. Initially the minimum distance between nodes is assumed to be r_{min}, which satisfies $r_{min} < r_n$, although later this assumption will be dropped, letting $r_{min} \to 0$.

3. THE EFFECTS OF PATH LOSS

In the absence of fading, i.e. when the only propagation phenomenon considered is the path loss, the signal power is assumed to decay upon increasing the distance r according to $r^{-\alpha}$, yielding:

$$G(r) = r^{-\alpha}, \quad (2)$$

where r and $G(r)$ are the distance and the power gain between two nodes, respectively, and α is the path loss exponent. In general we have $2 \leq \alpha \leq 4$ in a typical path loss model [11].

Let us assume that node j is transmitting to node i roaming at a distance less than r_n. Owing to the central limit theorem, the interference may be assumed to be approximately Gaussian. Thus only the fluctuation of the received signal power is considered.

In the model of [1], the guard zone[5] is appropriately selected to guarantee that all nodes' transmissions to other nodes roaming at a distance less than r_n achieve the minimum required SINR β, so that we have $\gamma_{ji} = \beta\left(\frac{r_n}{r_{ji}}\right)^{\alpha}$.

[5]A guard zone is specified as a transmission exclusion zone imposed for the sake of preventing a neighbouring node from transmitting on a channel already activated within the zone at the same time.

In the model of [1], the transmission rate is fixed. Hence the throughput c_g achievable without *rate adaptation* is also fixed and determined by the Shannon limit [10] at the minimum required SINR β, yielding $c_g = W\log_2(1+\beta)$.

Since node j is randomly and uniformly distributed in $\mathcal{S}$, furthermore, given that r_{ji} is less than the reliable range of transmission r_n, the conditional Probability Density Function (PDF) of the distance r_{ji} and the conditional PDF of the SINR γ_{ji} can be shown to be:

$$f_{r|r<r_n}(r_{ji}) = \frac{2r_{ji}}{r_n^2 - r_{min}^2}, \quad r_{min} < r_{ji} < r_n, \quad (3)$$

$$f_{\gamma|r<r_n}(\gamma_{ji}) = \frac{2\left(\frac{\gamma_{ji}}{\beta}\right)^{-\frac{2}{\alpha}-1}}{\alpha\beta\left[1-\left(\frac{r_{min}}{r_n}\right)^2\right]}, \quad \beta < \gamma_{ji}. \quad (4)$$

If perfect *rate adaptation* is available, the achievable average throughput c_a can be shown to be:

$$c_a = \frac{2W}{(r_n^2 - r_{min}^2)\ln 2}\int_{r_{min}}^{r_n} r_{ji}\ln\left[1+\beta\left(\frac{r_n}{r_{ji}}\right)^{\alpha}\right]\mathrm{d}r_{ji}. \quad (5)$$

Hence it is possible to estimate the achievable normalized per-node throughput improvement of $c_i = c_a/c_g$ attained with the advent of perfect *rate adaptation* by numerical integration. Upon substituting the normalized minimum distance of $u = r_{min}/r_n$ between *ad hoc* nodes as well as the normalized distance $s = r_{ji}/r_n$ into Equation 5, we arrive at the following theorem quantifying the normalized per-node throughput improvement in the absence of fading.

Theorem 1

$$\begin{aligned} c_i &= \frac{c_a}{c_g} = \frac{2\int_u^1 s\ln(1+\beta s^{-\alpha})\mathrm{d}s}{(1-u^2)\ln(1+\beta)} \leq \frac{2\int_0^1 s\ln(1+\beta s^{-\alpha})\mathrm{d}s}{\ln(1+\beta)} \\ &= c_i^0 < +\infty, \end{aligned} \quad (6)$$

where the upper bound c_i^0 is the maximum achievable normalized throughput improvement c_i attained with the advent of perfect rate adaptation, when we have $r_{min} = 0$. □

Note in Equation 6 that the upper bound c_i^0 is a constant that is independent of n, and it is determined purely by the propagation parameters, α and β. Therefore, it is concluded that c_a has the same order as c_g, which is the achievable per-node throughput in the model of [1]. In other words, even perfect *rate adaptation* fails to change the scaling law of the achievable per-node throughput result of [1].

Figures 1 and 2 show that the achievable normalized per-node throughput improvement c_i is a decreasing function of the normalized minimum distance r_{min}/r_n. In other words, as the minimum distance between nodes decreases, the achievable normalized per-node throughput improvement increases, because the link quality fluctuation becomes larger at a smaller normalized minimum distance between nodes, while *fixed rate transmission* fails to efficiently exploit the available capacity, when the link quality is improved.

4. THE EFFECTS OF SHADOW FADING

If the effects of shadowing are taken into account, the shadow-faded power gain is log-normally distributed with a mean given by Equation 2. Then the conditional PDF of the shadow-faded power gain at a certain distance is given by [11]:

$$f_{G|r}(G) = \frac{1}{\sqrt{2\pi}\sigma G}e^{-\frac{(\ln G + \alpha\ln r)^2}{2\sigma^2}}, \quad (7)$$

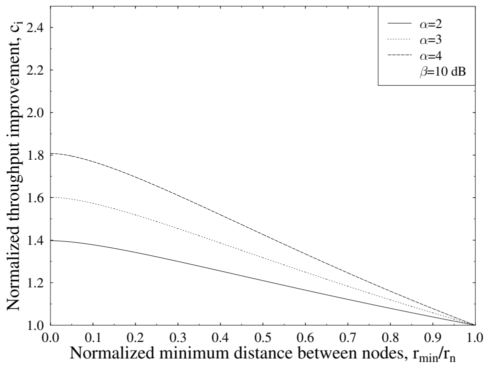

Figure 1: The normalized per-node throughput improvement c_i versus the normalized minimum distance r_{min}/r_n between nodes for different values of the path loss exponent α at a required SINR value of $\beta = 10$ dB in the absence of fading, which is computed from Equation 6.

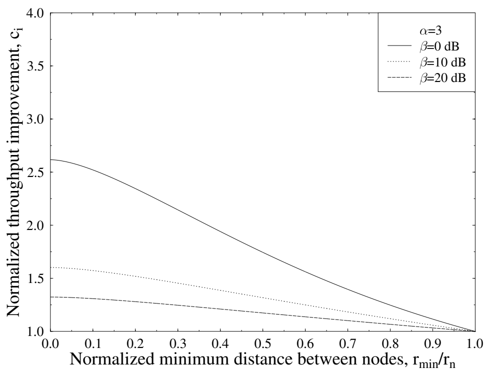

Figure 2: The normalized per-node throughput improvement c_i versus the normalized minimum distance r_{min}/r_n between nodes for different values of the required SINR β at a path loss exponent of $\alpha = 3$ in the absence of fading, which is computed from Equation 6.

where G and r are the power gain and the distance between two nodes, respectively and σ is the standard deviation of the lognormal shadowing in natural units. In practice the range of σ is $5 \sim 12$ dB and its typical value is 8 dB [11], i.e. we have $1.15 \sim 2.76$ and 1.84 in terms of natural units.

Owing to the central limit theorem, the interference is approximatively Gaussian distributed. Hence only the fluctuation of the shadow-faded received signal power is considered. The guard zone is appropriately selected to guarantee that all nodes' transmissions to other nodes roaming at a distance less than r_n achieve the minimum required SINR β on average, hence we have:

$$\gamma_{ji} = \beta r_n^{\alpha} G_{ji}, \tag{8}$$

where the shadow-faded power gain G_{ji} is log-normally distributed with a mean of $r_{ji}^{-\alpha}$.

Substituting Equation 8 into Equation 7 and applying the probability transformation formula [12], we have the conditional PDF of γ_{ji} at a given distance r_{ji}:

$$f_{\gamma|r_{ji}}(\gamma_{ji}) = \frac{1}{\sqrt{2\pi}\sigma\gamma_{ji}} e^{-\frac{(\ln\gamma_{ji}+\alpha\ln r_{ji}-\ln\beta-\alpha\ln r_n)^2}{2\sigma^2}}. \tag{9}$$

Upon substituting Equation 3 into Equation 9 and applying the theorem of total probability [12], we arrive at the PDF of γ_{ji} conditioned on $r_{ji} < r_n$:

$$f_{\gamma|r_{ji}<r_n}(\gamma_{ji}) = \frac{2\int_{r_{min}}^{r_n} r_{ji} e^{-\frac{(\ln\gamma_{ji}+\alpha\ln r_{ji}-\ln\beta-\alpha\ln r_n)^2}{2\sigma^2}} \mathrm{d}r_{ji}}{\sqrt{2\pi}\sigma\gamma_{ji}(r_n^2 - r_{min}^2)}. \tag{10}$$

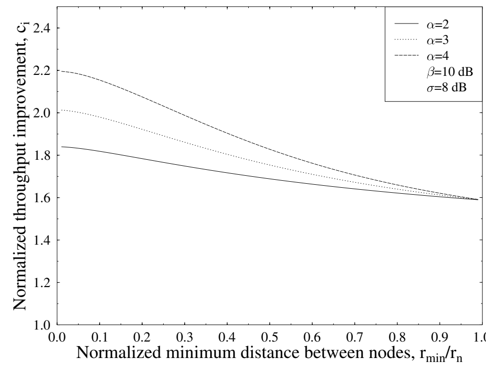

Figure 3: The normalized per-node throughput improvement c_i versus the normalized minimum distance r_{min}/r_n between nodes for different values of the path loss exponent α at a required SINR value of $\beta = 10$ dB and a lognormal shadowing standard deviation of $\sigma = 8$ dB in the presence of shadow fading, which is computed from Equation 12.

Therefore the normalized per-node throughput improvement c_i achieved with the aid of perfect *rate adaptation* may be expressed as follows:

$$c_i = \frac{c_a}{c_g} = \frac{\int_{\beta}^{\infty} f_{\gamma|r<r_n}(\gamma_{ji})\ln(1+\gamma_{ji})\mathrm{d}\gamma_{ji}}{\ln(1+\beta)\int_{\beta}^{\infty} f_{\gamma|r<r_n}(\gamma_{ji})\mathrm{d}\gamma_{ji}}. \tag{11}$$

Upon substituting the logarithmic normalized minimum distance of $u = \ln r_{min} - \ln r_n$ between *ad hoc* nodes as well as the logarithmic normalized distance of $s = \ln r_{ji} - \ln r_n$ and the logarithmic normalized SINR of $t = \ln\gamma_{ji} - \ln\beta$ into Equation 11, we arrive at the following theorem in the presence of shadow fading.

Theorem 2

$$\begin{aligned} c_i &= \frac{\int_0^{+\infty}\ln(1+\beta e^t)\mathrm{d}t\int_u^0 e^{2s}e^{-\frac{(t+\alpha s)^2}{2\sigma^2}}\mathrm{d}s}{\ln(1+\beta)\int_0^{+\infty}\mathrm{d}t\int_u^0 e^{2s}e^{-\frac{(t+\alpha s)^2}{2\sigma^2}}\mathrm{d}s} \\ &\le \frac{\int_0^{+\infty}\ln(1+\beta e^t)\mathrm{d}t\int_{-\infty}^0 e^{2s}e^{-\frac{(t+\alpha s)^2}{2\sigma^2}}\mathrm{d}s}{\ln(1+\beta)\int_0^{+\infty}\mathrm{d}t\int_{-\infty}^0 e^{2s}e^{-\frac{(t+\alpha s)^2}{2\sigma^2}}\mathrm{d}s} \\ &= c_i^0 < +\infty, \end{aligned} \tag{12}$$

where the upper bound c_i^0 experienced in the presence of shadow fading is the maximum achievable normalized throughput improvement c_i attained with the advent of perfect rate adaptation, when we have $r_{min} = 0$. □

Observe in Equation 12 that the upper bound c_i^0 is still a constant, regardless of the specific value of n, and it is purely determined by the propagation parameters α, β and σ. Therefore, it is concluded that c_a has the same order as c_g, which is the achievable throughput in the model of [1]. In other words, perfect *rate adaptation* fails to change the scaling law of the per-node throughput result of [1], even in the presence of shadow fading.

Figures 3 - 5 show that the achievable normalized per-node throughput improvement c_i experienced in the presence of shadow fading is also a decreasing function of the normalized minimum distance r_{min}/r_n, and this trend is similar to that in the absence of shadowing, as it was evidenced by Figures 1 and 2. However, the achievable normalized per-node throughput improvement c_i is higher than unity even at $r_{min}/r_n = 1$, which is different from that in the absence of shadowing. This

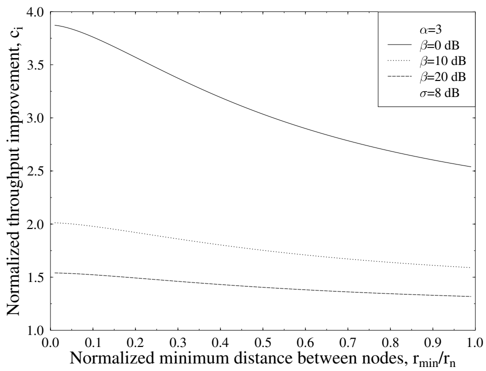

Figure 4: The normalized per-node throughput improvement c_i versus the normalized minimum distance r_{min}/r_n between nodes for different values of the required SINR β at a path loss exponent value of $\alpha = 3$ and a lognormal shadowing standard deviation of $\sigma = 8$ dB in the presence of shadow fading, which is computed from Equation 12.

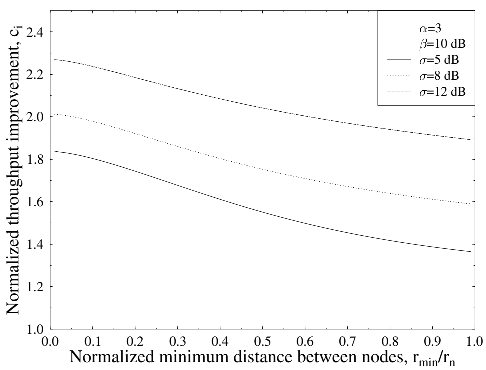

Figure 5: The normalized per-node throughput improvement c_i versus the normalized minimum distance r_{min}/r_n between nodes for different values of the lognormal shadowing standard deviation σ at a path loss exponent value of $\alpha = 3$ and a required SINR of $\beta = 10$ dB in the presence of shadow fading, which is computed from Equation 12.

gain was achieved by counteracting the link quality variation imposed by shadow fading, regardless of the normalized node separation. Observe in Equation 12 that at $r_{min}/r_n = 1$ we have:

$$c_i|_{\frac{r_{min}}{r_n}=1} = \frac{\int_0^{+\infty} \ln(1+\beta e^t) e^{-\frac{t^2}{2\sigma^2}} \mathrm{d}t}{\ln(1+\beta) \int_0^{+\infty} e^{-\frac{t^2}{2\sigma^2}} \mathrm{d}t} > 1. \quad (13)$$

We observe from Equation 13 that the normalized per-node throughput improvement c_i achieved at $r_{min}/r_n = 1$ is independent of the path loss exponent α, and it is purely determined by the required minimum SINR β as well as the lognormal shadowing standard deviation σ. This is because the conditional PDF of γ_{ji} at a given distance r_{ji} does not depend on α at $r_{min} = r_n$, as observed in Equation 9. Hence the curves associated with different values of α in Figure 3 converge, when we have $r_{min} \to r_n$, but this is not the case for different values of β, as seen in Figure 4 or for different values of σ, as portrayed in Figure 5.

5. EXAMPLE: AQAM

The family of AQAM schemes constitutes an efficient *rate adaptation* technique designed with low complexity in mind for the sake of increasing the achievable throughput [13]. There are several criteria that may be invoked for choosing the switching levels between the adjacent AQAM modes [13, 14]. In the previous sections we used the idealized concept of instantaneous SINR channel quality knowledge for evaluating the beneficial effects of perfect *rate adaptation* on the achievable effective throughput upper bound.

In this section a K-mode adaptive square QAM scheme using Gray coding is investigated. The mode selection rule is formulated as follows [14]:

Choose mode k, when we have $s_k \leq \gamma_s < s_{k+1}, k \in \{0, ..., K\}$,

where γ_s is the instantaneous SNR per symbol, s_k is the kth switching level and $s_0 = 0$, $s_{K+1} = \infty$. The AQAM constellation size is given by M_k phasors in mode k as follows:

$$M_0 = 0, \qquad M_1 = 2, \qquad M_k = 2^{2(k-1)}, k = 2, ..., K.$$

The number of bits per symbol (BPS) b_k transmitted in mode k is given by:

$$b_0 = 0, \qquad b_k = \log_2 M_k, k = 1, ..., K.$$

The general BER expression of M-ary square QAM using Gray coding is given by Equation 14 and 16 in [15], where $\gamma = \frac{\gamma_s}{\log_2 M}$ is the SNR per bit. Hence we arrive at the AQAM parameters listed in Table 1, which are independent of the associated SNR distribution. For example, if a 5-mode square AQAM scheme is adopted, the maximum constellation size will be $M_5 = 256$ and the highest switching level becomes $s_6 = \infty$, regardless of the target BER.

The average number of bits per symbol normalized to that of the fixed rate BPSK scheme is [14]:

$$B_i = \frac{\sum_{k=1}^{K} b_k \int_{s_k}^{s_{k+1}} f_{\gamma_s}(\gamma_s) \mathrm{d}\gamma_s}{B_{\mathrm{BPSK}}}, \quad (14)$$

where $f_{\gamma_s}(\gamma_s)$ is the PDF of the SNR per symbol and B_{BPSK} is the BPS throughput of the fixed rate BPSK scheme. In general a constant symbol rate is used in AQAM, regardless of the modulation mode selected, hence a constant bandwidth is required. Again, if we treat the co-channel interference as noise, which is justified by the central limit theorem, $f_{\gamma_s}(\gamma_s)$ is given by Equations 4 and 10 in the absence and in the presence of shadowing, respectively. The PDFs of their normalized values associated with $r_{min} = 0$ are depicted in Figure 6. Since the SINR achieved at the fringes of the transmission range r_n exactly satisfies the minimum SINR requirement β, provided that only the effect of path loss is considered, the SINR normalized to β is always higher than or equal to 0 dB in the absence of fading, as suggested by Figure 6. The peak value of the SINR PDF is reached at a normalized SINR value of less than 0 dB in the presence of shadowing, because the abscissa value of the peak $r^{-\alpha} e^{-\sigma^2}$ of the lognormal distribution in Equation 7 is less than the SINR's mean value of $r^{-\alpha} e^{-\sigma^2/2}$. The achievable normalized average BPS throughput B_i versus the number of modes K of K-mode square AQAM systems associated with $r_{min} = 0$ and $\beta = s_1$ is characterized in Figure 7, which was recorded both in the absence of fading and in the presence of shadowing.

Figure 7 shows that AQAM is capable of substantially improving the average BPS throughput both in the absence of fading and in the presence of shadowing compared to the fixed rate BPSK scheme. However, the additional throughput improvement achieved by a high-complexity scheme using more than four AQAM modes is marginal, because the probability of activating the high-BPS modes drops exponentially, when the SINR normalized to β increases, as suggested by the PDF seen in Figure 6. This result is in line with Theorem 1 and Theorem 2, suggesting that even perfect *rate adaptation* is incapable of improving the scaling law of the per-node throughput

k	0	1	2	3	4	5	6
M_k	0	2	4	16	64	256	1024
b_k	0	1	2	4	6	8	10
s_k(dB) BER $= 10^{-3}$	$-\infty$	6.7895	9.7998	16.5430	22.5490	28.4147	34.2607
s_k(dB) BER $= 10^{-5}$	$-\infty$	9.5879	12.5982	19.4551	25.5684	31.5341	37.4728
mode	No Tx	BPSK	QPSK	16-QAM	64-QAM	256-QAM	1024-QAM

Table 1: The parameters of K-mode square AQAM systems using Gray coding and designed for maintaining BER $= 10^{-3}$ and 10^{-5}, respectively. The switching thresholds were evaluated from Equations 14, 16 in [15] and $\gamma = \gamma_s / \log_2 M$.

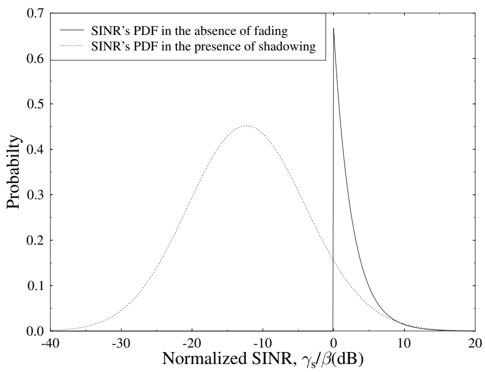

Figure 6: The PDFs of the SINRs normalized to the minimum SINR requirement β both in the absence of fading and in the presence of log-normal shadowing having $\alpha = 3$ and $\sigma = 8$ dB, which were computed from Equations 4 and 10 for $r_{min} = 0$, respectively.

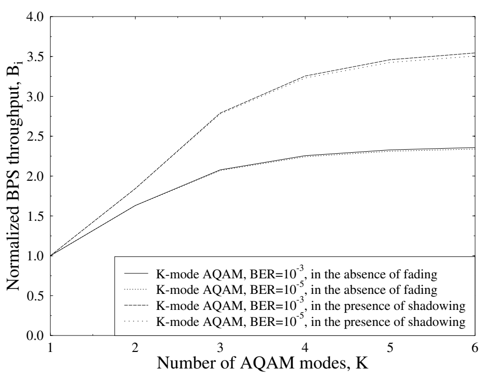

Figure 7: The achievable normalized per-node average BPS throughput B_i versus the number of modes K in K-mode square AQAM systems using Gray coding for a path loss exponent value of $\alpha = 3$, a lognormal shadowing standard deviation of $\sigma = 8$ dB and a target BER of 10^{-3} and 10^{-5}, respectively, recorded both in the absence of fading and in the presence of shadow fading in a random *ad hoc* network. The PDF $f_{\gamma_s}(\gamma_s)$ of the SNR per symbol is given by Equation 10 and Equation 10, respectively.

attained either in the absence of fading or in the presence of shadowing. The achievable normalized average BPS throughput recorded in the case of a higher threshold set designed for maintaining BER $\geq 10^{-5}$ is only marginally lower than that in the case of a lower threshold set designed for maintaining BER $\geq 10^{-3}$, since the distributions of the normalized SINR of the BER $= 10^{-5}$ and 10^{-3} scenarios are identical, as seen in Figure 6. This implies that a lower BPS throughput improvement may be achieved in case of requiring a lower BER of 10^{-5}, which conforms to the trends observed in Figure 2. However, it does not imply that the AQAM scheme achieves a lower BPS throughput in the case of aiming for a lower instantaneous BER, since we normalize the BPS throughput to that of the fixed rate BPSK scheme, which is different for the scenarios of BER $= 10^{-3}$ and BER $= 10^{-5}$ owing to the different values of r_n.

6. CONCLUSION

In this paper we have focused our attention on the effects of *rate adaptation* on the achievable throughput of random *ad hoc* networks, which was discussed in the context of both path loss and shadow fading. In conclusion, perfect *rate adaptation* has the potential of considerably improving the achievable throughput of the random *ad hoc* network compared to *fixed rate transmissions*, since *rate adaptation* is capable of mitigating the effects of link quality fluctuations, as shown in Figures 1 - 5. However, Theorem 1 and 2 revealed that even perfect rate control fails to change the scaling law of the per-node throughput result given by $\Theta\left(\frac{1}{\sqrt{n \log n}}\right)$ in [1], regardless of the absence or presence of shadow fading. This conclusion was further confirmed by Figure 7 in the context of our AQAM examples. The maximum normalized throughput improvement c_i^0 achieved with the aid of perfect *rate adaptation* is determined purely by the path loss exponent α, the required minimum SINR β and the lognormal shadowing standard deviation σ. We observed in Figures 1, 3 and 5 that the achievable normalized throughput c_i^0 increases, as α or σ increases, because it is capable of efficiently mitigating the link quality variations. More explicitly, this was demonstrated in Figure 1 in the absence of fading, while in Figures 3 and 5 in the presence of shadowing, respectively. By contrast, c_i^0 decreases as β decreases, as a consequence of the reduced marginal channel throughput, as shown in Figure 2 in the absence of fading and in Figure 4 in the presence of shadowing, respectively.

7. REFERENCES

[1] P. Gupta and P. Kumar, "The capacity of wireless networks," *IEEE Transactions on Information Theory*, vol. 46, pp. 388–404, March 2000.

[2] A. Spyropoulos and C. Raghavendra, "Capacity bounds for ad-hoc networks using directional antennas," in *IEEE International Conference on Communications*, vol. 1, (Anchorage, Alaska, USA), pp. 348–352, 11-15 May 2003.

[3] A. Spyropoulos and C. Raghavendra, "Asympotic capacity bounds for ad-hoc networks revisited: the directional and smart antenna cases," in *IEEE Global Telecommunications Conference*, vol. 3, (San Francisco, California, USA), pp. 1216–1220, 1-5 December 2003.

[4] R. Ramanathan and J. Redi, "A brief overview of ad hoc networks: challenges and directions," *IEEE Communications Magazine*, vol. 40, pp. 20–22, May 2002.

[5] M. Grossglauser and D. Tse, "Mobility increases the capacity of ad hoc wireless networks," *IEEE/ACM Transactions on Networking*, vol. 10, pp. 477–486, August 2002.

[6] D. S. Heberto del Rio, "Logarithmic expected packet delivery delay in mobile ad hoc wireless networks," *Wiley Journal on Wireless Communications and Mobile Computing*, vol. 4, pp. 281–287, May 2004.

[7] B. Liu, Z. Liu, and D. Towsley, "On the capacity of hybrid wireless networks," in *IEEE INFOCOM*, vol. 2, (San Francisco, Carlifornia, USA), pp. 1543 –1552, 30 March-3 April 2003.

[8] U. C. Kozat and L. Tassiulas, "Throughput capacity of random ad hoc networks with infrastructure support," in *International Conference on Mobile Computing and Networking*, (San Diego, Carlifornia, USA), pp. 55–65, 14-19 September 2003.

[9] S. Toumpis and A. J. Goldsmith, "Capacity regions for wireless ad hoc networks," *IEEE Transactions on Wireless Communications*, vol. 2, pp. 736–748, July 2003.

[10] T. M. Cover and J. A. Thomas, *Elements of information theory*. John Wiley, 1991.

[11] J. G. Proakis, *Digital Communications*. McGraw-Hill Companies, Inc., 4th ed., 2001.

[12] E. Lloyd, *Probability*, vol. II of *Handbook of Applicable Mathematics*. John Wiley & Sons Ltd., 1980.

[13] L. Hanzo, S. X. Ng, T. Keller, and W. Webb, *Quadrature Amplitude Modulation: From Basics to Adaptive Trellis-Coded, Turbo-Equalised and Space-Time Coded OFDM, CDMA and MC-CDMA Systemss*. John Wiley & Sons Ltd., 2 ed., November 2004.

[14] B. Choi and L. Hanzo, "Optimum mode-switching-assisted constant-power single- and multicarrier adaptive modulation," *IEEE Transactions on Vehicular Technology*, vol. 52, pp. 536–560, May 2003.

[15] K. Cho and D. Yoon, "On the general BER expression of one- and two-dimension amplitude modulations," *IEEE Transactions on Communications*, vol. 50, pp. 1074–1080, July 2002.